

## Probing the Superconducting Proximity Effect in NbSe<sub>2</sub> by Scanning Tunneling Microscopy

S. H. Tessmer,\* M. B. Tarlie,† D. J. Van Harlingen, D. L. Maslov,‡ and P. M. Goldbart

*Department of Physics and Materials Research Laboratory, University of Illinois at Urbana-Champaign, 1110 West Green Street, Urbana, Illinois 61801*

(Received 5 June 1995)

Cryogenic scanning tunneling microscopy has been used as a local probe of the superconducting proximity effect across a normal metal–superconductor interface of a short coherence length superconductor. Both the topography and the local electronic density of states were measured on a superconducting NbSe<sub>2</sub> crystal decorated with nanometer-size Au islands. The presence of a quasiparticle bound state could be inferred even when the probe was located directly on the bare NbSe<sub>2</sub> surface near an Au island, indicating a severe depression of the pair potential inside the superconductor due to the proximity effect. [S0031-9007(96)00754-5]

PACS numbers: 74.50.+r

Cryogenic scanning tunneling microscopy (STM) has the unique spectroscopic capability to resolve the local electronic density of states  $N(E, \mathbf{r})$  with sub-meV energy sensitivity and atomic spatial resolution. This provides a novel probe of inhomogeneous superconducting structures, of which the normal metal ( $N$ ) to superconductor ( $S$ ) planar interface is the most basic configuration. If the electrical contact between the two metals is good, superconductivity is weakened in  $S$  and induced in  $N$ . The phenomenon, known as the proximity effect, is typically described by a spatially varying superconducting condensate amplitude  $F$ , which varies over the length scales  $\xi_S$  in  $S$  and  $\xi_N$  in  $N$  [1].  $F$  is related to the pair potential  $\Delta = gF$  by the effective pairing interaction constant  $g$ . The proximity effect in layered superconductors, such as NbSe<sub>2</sub> and the high- $T_c$  cuprates, presents new experimental and theoretical challenges, in part because  $\xi_S$  does not greatly exceed the Fermi wavelength  $2\pi/k_F$ . Recent STM measurements on Au in contact with NbSe<sub>2</sub> showed that the magnitude of  $\Delta$  inside the Au is nearly zero relative to the bulk NbSe<sub>2</sub> value, even for extremely thin (6 Å) Au layers [2]. This observation is consistent with recent calculations [3,4]. The reduction in  $\Delta$  creates a potential well for quasiparticles resulting in a quasiparticle bound state, as first described by de Gennes and Saint-James [5]. These are localized states bound by Andreev reflection at the  $NS$  interface and ordinary reflection at the  $N$ /vacuum boundary.

In this Letter we report STM measurements that probe the proximity effect directly by resolving the local electronic density of states in and near small Au islands in good electrical contact with the bulk superconductor  $2H$ -NbSe<sub>2</sub>. The STM allows us to characterize the proximity effect inside a thick superconductor at a much smaller length scale than can be achieved by conventional techniques using tunnel junctions, proximity-effect sandwiches, or point contacts. We observe a bound state not only in the Au islands as previously reported [2], but also when tunneling into the bare NbSe<sub>2</sub> surface between islands. By sampling the energy and spatial dependence of the bound state, we infer

the spatial variation of  $\Delta$  both perpendicular and parallel to the interface. We find that beneath the Au islands  $\Delta$  is severely suppressed on the  $S$  side of the interface to no more than 10% of its bulk value. This layer of suppressed pair potential dominates the bound state formed at the  $NS$  interface, and extends laterally to allow a bound state on the bare superconductor surface as well. This is in contrast to the conventional picture of the proximity effect in which the effect of a thin normal overlayer is expected to be small. We note that previous STM experiments near Nb/InAs interfaces observed a spatial modification of the tunneling spectra that was attributed to the proximity effect, but these experiments were not capable of resolving bound quasiparticle states [6].

The Au-NbSe<sub>2</sub> system provides an ideal environment for the STM study of the proximity effect because both materials are chemically inert and can form a clean, sharp, planar interface. Au exhibits no superconductivity, while NbSe<sub>2</sub> is a well-characterized, anisotropic, layered superconductor which undergoes a BCS transition at  $T_c = 7.2$  K with an energy gap  $\Delta_\infty = 1.3$  meV and coherence lengths  $\xi_{S\perp} = 23$  Å and  $\xi_{S\parallel} = 77$  Å perpendicular and parallel to the layers, respectively [7]. To minimize surface contamination, the samples are prepared in a customized STM system that allows for *in situ* sample preparation [8]. Crystals of NbSe<sub>2</sub> (typically 4 mm × 4 mm × 0.2 mm) are freshly cleaved prior to thermal evaporation of Au with a nominal thickness of 2 Å, as measured by a crystal monitor. Topographic and spectroscopic measurements are taken with the STM immersed in liquid helium at a temperature  $T = 1.6$  K. The deposited Au forms distinct islands of widths 40 to 100 Å separated by gaps of 20 to 100 Å in which the atomic lattice of NbSe<sub>2</sub> can be imaged. Tunneling spectra are obtained in the standard way by using a lock-in amplifier to measure the differential conductance  $dI/dV$  vs  $V$  while holding the STM tip (chemically etched Pt-Ir) fixed at location  $\mathbf{r}$  thus providing a probe of  $N(eV, \mathbf{r})$ . Data are normalized to the conductance at high voltage; typical tunneling resistances are  $\sim 10^8 \Omega$ .

All spectra taken in the vicinity of different Au islands show qualitatively similar behavior. Here we report tunneling spectra sampled at a series of locations on and near one of the larger Au islands, shown in Fig. 1(a). Spectra were taken at 25 Å increments along the path indicated. In Fig. 1(c), we show a sequence of six spectra. The first five were taken at the locations A through E indicated in Fig. 1(b), sampling different points on the island from the highest point (A), defined as  $x = 0$ , down to the bare NbSe<sub>2</sub> surface off the island (D, E). The sixth spectrum was taken on a pure NbSe<sub>2</sub> sample without any Au, and serves as a reference. At all locations, we see a gaplike spectrum with a pronounced dip in the density of states at the Fermi energy ( $eV = 0$ ) and peaks on both sides. All of the spectra on the Au-decorated sample exhibit an enhancement in the conductance both at zero voltage and at the peaks compared to the pure NbSe<sub>2</sub> spectrum. Although the local Au thickness varies substantially, the spectra are found to be nearly independent of position and, hence, the thickness, showing only a variation in the zero-voltage conductance of about 10% and a shift in the peak voltage of about 0.2 mV.

To analyze the data, we begin with the usual assumption that the measured spectra represent the convolution of the true density of states with a smearing function. We have found it convenient to describe the smearing by using the Fermi distribution with an elevated effective temperature  $T^* > T$ , intended to account phenomenologically for the anisotropy in the energy gap [9,10] and nonthermal energy smearing typically observed in STM spectra that likely arises from external rf noise. For pure NbSe<sub>2</sub>, this procedure yields excellent fits to a BCS density of states with  $\Delta_\infty = 1.3$  meV, as shown in Fig. 1(c). In contrast, we find that, for Au-decorated samples, the

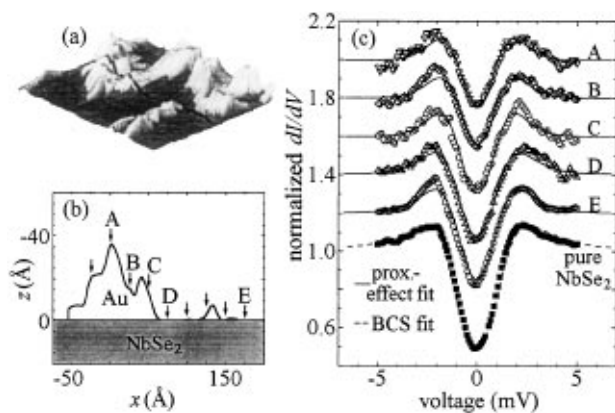


FIG. 1. (a) A 250 Å × 200 Å topographic image of the sample surface. The black curve indicates the path along which spectra were taken, which is shown in profile in (b). (c) A series of five spectra from the highest point on the Au (A) down to the NbSe<sub>2</sub> substrate (D, E). Solid curves are fits based on our proximity-effect model. The bottom curve is a representative spectrum of pure NbSe<sub>2</sub> samples, shown fit to the BCS density of states. The successive curves have been shifted upward for clarity.

BCS form (for any choice of  $\Delta_\infty$  and  $T^*$ ) cannot adequately fit the tunneling spectra taken either directly on the islands or on the bare NbSe<sub>2</sub> surface near the islands. We believe that the discrepancy arises from the proximity effect of the Au islands which suppresses  $\Delta$ , creating a potential well that supports a quasiparticle bound state. The  $\Delta$  suppression extends even into regions between Au islands because of the nonlocality of the pair potential. The bound state contributes a peak in the density of states at the bound state energy that accounts for the excess conductance near the gap edge.

Our basic approach is to estimate the spatial profile of  $\Delta$  in the vicinity of an island by fitting the measured tunneling spectra to solutions of the Bogoliubov–de Gennes equations for a trial profile. In lieu of an involved three-dimensional calculation, we use the following tractable phenomenological model. We assume that the profile of  $\Delta$  can be parametrized in the following quasi-one-dimensional form inside the superconductor:

$$\Delta(x, y, z)|_{z>0} = \Delta_\infty \tanh\left[\frac{z + z_0(x, y)}{\sqrt{2} \xi_{S\perp}}\right] \quad (1)$$

and set  $\Delta = 0$  inside the normal-metal layer of thickness  $d_N$ , as shown in Fig. 2(a). The length  $z_0$  characterizes the reduction of  $\Delta$  inside the superconductor. It is related to the value of  $\Delta$  on the S side of the interfacial plane,  $\Delta_0(x, y) = \Delta_\infty \tanh[z_0(x, y)/\sqrt{2} \xi_{S\perp}]$ , which is a convenient parameter to characterize the magnitude of the proximity suppression in S. The resulting pair-potential well extends into the NbSe<sub>2</sub>. Consequently, the strength

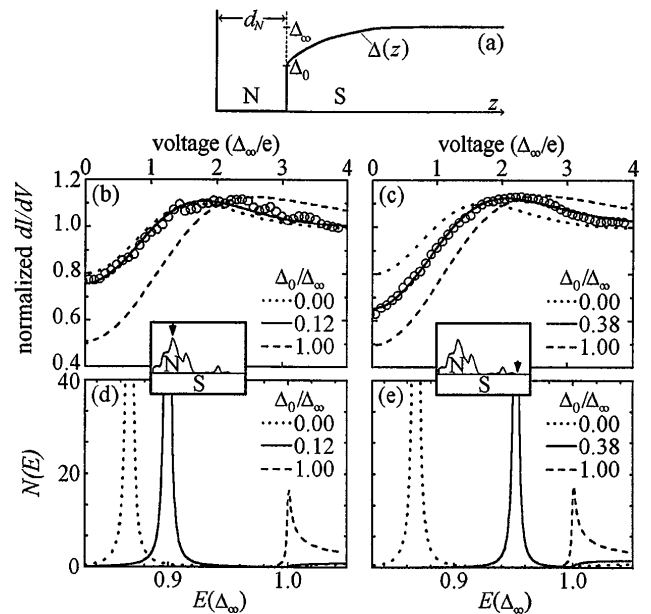


FIG. 2. (a) Schematic of our proximity-effect model. (b), (c) Demonstration of the sensitivity of our fitting procedure to  $\Delta_0$ , with the best fits shown as the solid curves. (d), (e) The densities of states extracted from the (b), and (c) curves. The dominant  $\delta$ -function-like peaks imply the existence of bound quasiparticle states.

of the well, and, hence, the energy of the bound states, depend on both  $d_N(x, y)$  and  $\Delta_0(x, y)$ .

Although it is possible and somewhat illuminating to compute the density of states from the Bogoliubov-de Gennes equations by directly assuming a form for the pair potential [11] or self-consistently [12], these procedures are complicated and computationally lengthy. Instead, we have developed an efficient Green function algorithm for solving the Gor'kov equations numerically for an arbitrary one-dimensional profile  $\Delta(z)$  that yields an acceptable approximation to the electronic density of states. Our approach is to approximate the smoothly varying pair potential by a sequence of step functions (typically 50), and calculate the surface density of states using a technique similar to that developed for a single-step pair potential [13]. Our model includes distinct Fermi velocities  $v_{FN}$  and  $v_{FS}$  and effective masses  $m_N$  and  $m_S$  for the  $N$  and  $S$  layers to account for differences in their electronic structures. The calculated density of states is then thermally broadened by an effective temperature  $T^*$  and fit to the experimental tunneling spectra by adjusting only the two parameters  $T^*$  and  $\Delta_0$ , the gap value on the  $S$  side of the interface.

We have applied our proximity-effect model to the measured spectra at each sampled location, using the measured topographical height  $d_N(x, y)$  above the NbSe<sub>2</sub> surface, and the following superconducting parameters for NbSe<sub>2</sub>:  $\Delta_\infty = 1.3$  meV,  $\xi_{S\perp} = 23$  Å, and  $E_{FS}/\Delta_\infty = 100$ . We also used material parameters characteristic of the Au-NbSe<sub>2</sub> system:  $v_{FS}/v_{FN} = 0.01$  [14] and  $m_S/m_N = 2.76$  [15], but the results are actually rather insensitive to these ratios since  $v_{FS} \ll v_{FN}$  and  $m_S \approx m_N$ . The values of  $\Delta_0$  and  $T^*$  were determined by using a least-squares fit to the spectrum at each location. As shown in Fig. 1(c), reasonable fits to the measured spectra were obtained, with  $\Delta_0/\Delta_\infty$  varying from 0.08 to 0.38, as plotted in Fig. 3, and  $T^*$  nearly uniform in the range  $7.5 \pm 0.8$  K. Figures 2(b) and 2(c) illustrates the sensitivity of the calculated spectra to  $\Delta_0$  by comparing the best-fit (solid) curves to the dotted curves obtained with  $\Delta_0 = 0$  (complete suppression inside  $S$ ) and the dashed curves for  $\Delta_0 = \Delta_\infty$  (no suppression). At the summit of the island, location  $A$  [Fig. 2(b)], we see

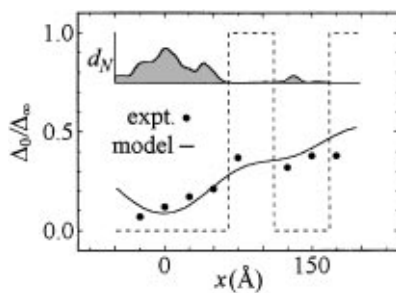


FIG. 3. Lateral dependence of  $\Delta_0$ . The experimental values (dots) are compared to a simple model (solid curve) based on the Au topography.

that the best fit is achieved at a surprisingly low value of  $\Delta_0 \approx 0.1\Delta_\infty$ . The  $\Delta_0 = \Delta_\infty$  curve, which corresponds to a pair-potential well contained entirely inside the Au, is clearly inadequate. Even at location  $E$  [Fig 2(c)], where the tunneling is directly into the bare superconductor,  $\Delta_0$  is substantially less than  $\Delta_\infty$ , indicating that the pair potential inside the superconductor is strongly suppressed by its proximity to the normal metal island.

The role of the  $\Delta$  suppression at the interface can be most clearly seen by removing the broadening from the calculated conductance curves, which yields an inferred density of states  $N(E)$ . This is shown in Figs. 2(d) and 2(e) for the spectra of Figs 2(b) and 2(c). We see that, at locations  $A$  and  $E$ , the best-fit  $N(E)$  (solid curves) are dominated by bound state peaks at  $0.89\Delta_\infty$  and  $0.95\Delta_\infty$ , respectively. Figure 2(e) also illustrates why the spectra cannot be adequately fit with the BCS density of states, corresponding in our model to  $\Delta_0 = \Delta_\infty$  and  $d_N = 0$ , which is shown as the dashed curve. The BCS peak, which arises from the enhanced density of scattering states near the gap edge, not only occurs at increased energy, but also has a height and shape in sharp contrast to the  $\delta$ -function-like bound-state peaks. Our modeling also predicts that the conductance spectra should have little dependence on the local Au thickness  $d_N$ , as we observe and in accordance with the expected behavior for very thin  $N$  layers [16]. In contrast, the spectra depend strongly on the magnitude of the  $\Delta$  suppression inside the superconductor, even though this suppression extends only to a depth of  $\xi_{S\perp}$ , which is comparable to  $d_N$ . This occurs because of the large mismatch in Fermi velocities between the Au and NbSe<sub>2</sub>, for which  $v_{FN}/v_{FS} \gg 1$ . As a result, the effective confinement wavelength in the normal region is of order  $h v_{FN}/\pi\Delta_\infty \gg d_N$ , whereas in the superconductor the effective wavelength would be of order  $h v_{FS}/\pi(\Delta_\infty - \Delta_0) \sim \xi_S$  in our model. The striking conclusion is that the bound state we observe, even where there is an Au overlayer, resides predominantly within the suppressed pair-potential region inside the NbSe<sub>2</sub>.

We now examine the spatial dependence of the pair potential in lateral directions. In all regions we probed, we found the same qualitative behavior shown in Fig. 3: the minimum  $\Delta_0$  (maximum  $\Delta$  suppression in  $S$ ) occurred directly beneath the islands, and the maximum  $\Delta_0$  (minimum suppression) occurred in the regions between islands. For an isolated Au island, the pair potential is expected to recover to the pure NbSe<sub>2</sub> limit of  $\Delta_0 = \Delta_\infty$  beyond the characteristic length scale  $L$  of the order  $\xi_{S\parallel}$  (77 Å) that measures the range of the proximity effect in the lateral direction. However, the lack of sufficient separation between islands prevented us from examining this limit directly. Instead, we deduce an approximate value for  $L$  from our data by using a simple model for  $\Delta_0(x, y)$ . Because, in the absence of lateral coherence,  $\Delta$  would only be suppressed directly beneath the Au islands, we first construct a simple function which has the constant

value  $\Delta_0^{\min}$  in regions covered with Au, but equals the full bulk gap  $\Delta_\infty$  elsewhere; a profile of the resulting discontinuous function is shown dashed in Fig. 3. The lateral proximity effect is then accounted for by broadening this function by convolution with a Gaussian distribution of width  $L$  in two dimensions,  $\exp[-2(x^2 + y^2)/L^2]$ . We apply this model to estimate  $\Delta_0(x)$  along the trajectory of Fig. 1(a). With the measured topography dictating the locations of the islands, only  $\Delta_0^{\min}$  and  $L$  are free parameters, determined by a least-squares fit to the data. We see that the results of the model, the solid curve in Fig. 3, is a reasonable fit to the measured values of  $\Delta_0(x)$ . The best-fit value for  $L$  is 81 Å, in good agreement with the accepted coherence length parallel to the layers  $\xi_{S\parallel} = 77$  Å that is expected to set the lateral length scale. The best-fit value for  $\Delta_0^{\min}$  is  $0.00\Delta_\infty$ , which indicates that a complete suppression of the pair potential would occur entirely inside the superconductor for a NbSe<sub>2</sub> crystal with a thin, continuous Au overlayer.

In light of our examination of the lateral dependence of  $\Delta_0$ , we conclude that the pair potential is almost completely suppressed inside NbSe<sub>2</sub> in contact with an Au overlayer. This is in sharp contrast to the standard theory of the proximity effect in which the value of  $\Delta$  on the  $S$  side of an  $NS$  interface is expected to be suppressed to  $\Delta_0 \approx \Delta_\infty[1 - \xi_S/(\xi_S + \xi_N)]$ , with even less suppression occurring for thin normal-metal layers for which  $d_N < \xi_N$ . For our system,  $\xi_{S\perp} = 23$  Å and  $\xi_N \sim 1$  μm so that suppression of no more than a few percent is expected. A self-consistent calculation following the conventional theory [3] does find a significant drop in  $\Delta$  of (20–30)% inside the NbSe<sub>2</sub>, but this is still considerably less than we observe. One plausible mechanism for the severe suppression of the order parameter at the interface follows from the fact that, for our superconductor,  $\xi_S$  does not greatly exceed  $1/k_F$ . In fact, perpendicular to the layers,  $1/k_F \approx 33$  Å [14] so that  $k_F\xi_S \approx 0.7$ . In the conventional picture [1], applicable only when  $k_F\xi_S \gg 1$ , the pair-potential  $\Delta$  has two distinct regions, a gradual suppression over the length  $\xi_S$  due to the leaking of the Cooper pairs out of the superconductor, i.e., the conventional proximity effect, and a sharp drop to zero at the interface over a length  $\xi_g \sim 1/k_F \ll \xi_S$  reflecting the profile of the effective pairing constant  $g$ . However, in the Au-NbSe<sub>2</sub> system,  $\xi_S \sim \xi_g$  so that a clear separation of these regions cannot be made. Therefore, we believe that the spatial variation of  $\Delta$  which we extract from our data combines both the conventional proximity suppression of  $\Delta$  and its modulation by the profile of  $g$ , enhancing the suppression of  $\Delta$  at the interface. This phenomenon should occur at interfaces with all short coherence length superconductors, in particular, the high- $T_c$  cuprates, and affect the properties of  $NS$  contacts and proximity-effect junctions.

In summary, we have performed local spectroscopic measurements across an  $NS$  interface with STM by prob-

ing small Au islands in contact with large superconducting NbSe<sub>2</sub> crystal. A quasiparticle bound state was observed even when tunneling directly into the NbSe<sub>2</sub>, evidence for a significant reduction of the superconductivity inside the NbSe<sub>2</sub> induced by the proximity of the Au overlayer. We are able to characterize these results by invoking a proximity-effect model to account for the vertical and lateral variation of the pair potential in the superconductor. We find that a severe suppression of the pair potential occurs inside the superconductor. These measurements give insight into the proximity effect in short coherence length superconductors.

We gratefully acknowledge beneficial conversations with A. J. Leggett, B. P. Stojkovic, H. F. Hess, L. H. Greene, and N. Hass, and the valuable technical assistance of J. W. Lyding, B. L. T. Ploufde, M. S. Wistrom, D. A. Wollman, and B. D. Yanoff. This work was supported by the National Science Foundation Materials Research Laboratory program (NSF-DMR89-20538) and by the Department of Energy (DEFG02-96ER45439).

---

\*Present address: Department of Physics, Massachusetts Institute of Technology, Cambridge, MA 02139.

†Present address: James Franck Institute, University of Chicago, Chicago, IL 60637.

‡On leave from the Institute for Microelectronics, Academy of Science, Chernogolovka, Russia 142432.

- [1] See G. Deutscher and P. G. Gennes, in *Superconductivity*, edited by R. D. Parks (Dekker, NY, 1969).
- [2] S. H. Tessmer, D. J. Van Harlingen, and J. W. Lyding, *Phys. Rev. Lett.* **70**, 3135 (1993).
- [3] B. Stojkovic and O. Valls, *Phys. Rev. B* **50**, 3374 (1994).
- [4] H. K. Im, E. A. Jagla, and C. A. Balseiro, *Phys. Rev. B* **50**, 10 117 (1994).
- [5] P. de Gennes and D. Saint-James, *Phys. Lett.* **4**, 151 (1963).
- [6] K. Inoue and H. Takayangi, *Phys. Rev. B* **43**, 6214 (1991).
- [7] P. de Trey, S. Gyax, and J. P. Jan, *J. Low. Temp. Phys.* **11**, 421 (1973).
- [8] S. H. Tessmer, D. J. Van Harlingen, and J. W. Lyding, *Rev. Sci. Instrum.* **65**, 2855 (1994).
- [9] H. F. Hess, in *Methods of Experimental Physics*, edited by J. Stroscio and W. Kaiser Scanning Tunneling Microscopy, Vol. 27 (Academic Press, Boston, 1993), pp. 432–434.
- [10] H. F. Hess, R. B. Robinson, and J. V. Waszczak, *Phys. Rev. Lett.* **64**, 2711 (1990).
- [11] F. Gygi and M. Schluter, *Phys. Rev. B* **41**, 822 (1990).
- [12] Y. Tanaka, H. Yamagami, and M. Tsukada, *Solid State Commun.* **79**, 349 (1991).
- [13] T. Wolfram, *Phys. Rev.* **170**, 481 (1968).
- [14] K. Takita *et al.*, *Physica (Amsterdam) C* **185C-189C**, 2717 (1991).
- [15] W. Y. Liang, *J. Phys. C* **6**, 551 (1973).
- [16] G. B. Arnold, *Phys. Rev. B* **18**, 1076 (1978).